# SIMULATION AND DESIGN OF THE COMPACT SUPERCONDUCTING CYCLOTRON C400 FOR HADRON THERAPY

Y. Jongen, M. Abs, A. Blondin, W. Kleeven, S. Zaremba, D. Vandeplassche, IBA, Belgium
V. Aleksandrov, S. Gursky, G. Karamysheva, N. Kazarinov, S. Kostromin, N. Morozov,
V. Romanov, N. Rybakov, A. Samartsev, E. Samsonov, G. Shirkov, V. Shevtsov, E. Syresin,
A. Tuzikov, JINR, Russia.

*Abstract*

Carbon therapy is a most effective method to treat the resistant tumors. A compact superconducting isochronous cyclotron C400 has been designed by IBA-JINR collaboration. This cyclotron will be used for radiotherapy with proton, helium and carbon ions. The $^{12}C^{6+}$ and $^{4}He^{2+}$ ions will be accelerated to the energy of 400 MeV/amu and will be extracted by electrostatic deflector, $H_2^+$ ions will be accelerated to the energy 265 MeV/amu and protons will be extracted by stripping. The magnet yoke has a diameter of 6.6 m, the total weight of the magnet is about 700 t. The designed magnetic field corresponds to 4.5 T in the hills and 2.45 T in the valleys. Superconducting coils will be enclosed in a cryostat; all other parts will be warm. Three external ion sources will be mounted on the switching magnet on the injection line located bellow of the cyclotron. The main parameters of the cyclotron, its design, the current status of development work on the cyclotron systems and simulations of beam dynamic will be presented.

## INTRODUCTION

Today, cancer is the second highest cause of death in developed countries. Its treatment still presents a real challenge. Protons and light ions allow depositing the radiation dose more precisely in a cancer tumor, reducing greatly the amount of dose received by healthy tissue surrounding the tumor with respect to electrons. But in addition to the ballistic accuracy of protons, light ion beams, like carbon beams have an extra advantage in radiation therapy: they have a different biological interaction with cells and are very effective even against some type of cancerous cells which resist to usual radiations. That is why the last years have seen increasing interest in particle therapy based on $^{12}C^{6+}$ ions. A C400 dedicated Carbon/Proton therapy cyclotron [1-4] (Fig. 1) has been designed by IBA-JINR collaboration.

Over the last 15 years IBA has designed and equipped over half of the clinical-based Proton Therapy (PT) facilities in the world. The new C400 cyclotron is derived from the design of the current PT C235 cyclotron and will be used for radiotherapy with proton, helium or carbon ions. The $^{12}C^{6+}$ and $^{4}He^{2+}$ ions will be accelerated to the energy 400 MeV/amu and extracted by an electrostatic deflector, $H_2^+$ ions will be accelerated to the energy 265 MeV/amu and extracted by stripping. All other ions with Q/M = 0.5, which can be produced in reasonable amount by current ECR ion sources, can be accelerated as well as for research purposes with unspecified intensity.
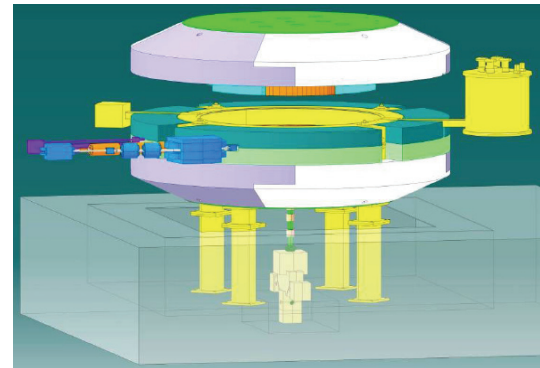


Figure 1: Common view of C400 cyclotron.

Table 1: Main parameters of the C400 Cyclotron

| General properties | |
|---|---|
| Accelerated particles | $H_2^+$, $^{4}He^{2+}$, $^{6}Li^{3+}$, $^{10}B^{5+}$, $^{12}C^{6+}$ |
| Injection energy | 25 keV/Z |
| Final energy of ions, protons | 400 MeV/amu 265 MeV |
| Extraction efficiency | ~70 % ( by deflector) |
| Number of turns | ~1700 |
| **Magnetic system** | |
| Total weight | 700 tons |
| Outer diameter | 6.6 m |
| Height | 3.4 m |
| Pole radius | 1.87 m |
| Valley depth | 60 cm |
| Bending limit | K = 1600 |
| Hill field | 4.5 T |
| Valley field | 2.45 T |
| **RF system** | |
| Radial dimension | 187 cm |
| Vertical dimension | 116 cm |
| Frequency | 75 MHz |
| Operation | 4th harmonic |
| Number of dees | 2 |
| Dee voltage: center extraction | 80 kV 170 kV |

The C400 design was based on the main cyclotron characteristics: compact design similar to the existing IBA C235 cyclotron; fixed energy, fixed field and fixed RF frequency (small RF frequency change 0.6% for $H_2^+$ regime set up); bending limit K=1600; accelerated particles $H_2^+$, $^4He^{2+}$, $^6Li^{3+}$, $^{10}B^{5+}$ and $^{12}C^{6+}$; superconducting coils enclosed in cryostat, all other parts are warm; axial injection using a spiral inflector; extraction of carbon beam with an electrostatic deflector; extraction of $H_2^+$ beam by stripping. All operating parameters of the C400 cyclotron are fixed now (Table 1).

The required isochronous magnetic field is shaped by axial and azimuth profiling of the sectors. The optimized sector geometry provides vertical focusing $Q_z{\sim}0.4$ in the region of extraction. Four-fold symmetry and spiral sectors with an elliptical gap (120 mm at the center decreasing to 12 mm at the extraction) provide stable beam acceleration up to 10 mm from the pole edge. Keeping the last orbit as close as possible to the pole edge facilitates extraction. Detailed dynamic simulations were performed to be sure that resonances crossed during acceleration did not cause significant harmful effect to the beam. The number of turns is expected to be about 1700.

## INJECTION

Three external ions sources are mounted on the switching magnet on the injection line located below of the cyclotron. $^{12}C^{6+}$ are produced by a high performance ECR at current 3 µA, alphas and $H_2^+$ are also produced by a simpler ECR source. All species have a Q/M ratio of 1/2 and all ion sources are at the same potential, so that small retuning of the frequency and a very small magnetic field change achieved by different excitation of 2 parts in the main coil are needed to switch from $H_2^+$ to alphas or to $^{12}C^{6+}$. We expect that the time to switch species will be not longer than two minutes, like the time needed to retune the beam transport line between different treatment rooms.
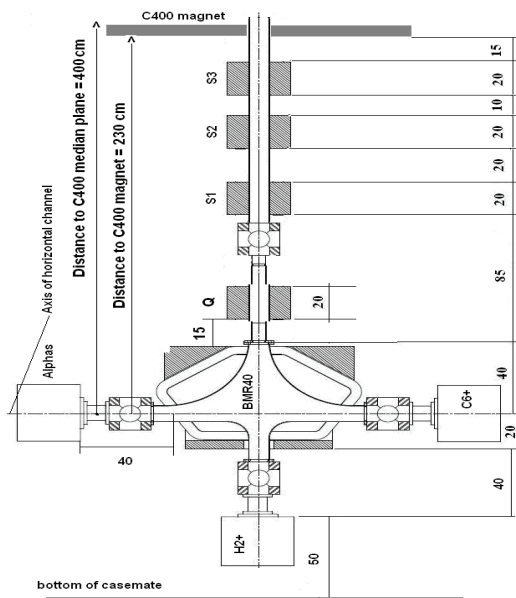


Figure 2: Scheme of the injection beam line.

Focusing in the channel (Fig. 2) is provided by three solenoid lenses (S1 … S3), the rotational symmetry of the beam is reestablished with the help of one quad Q placed just behind the BMR40 bending magnet. The 90º bending magnet has two horizontal entrances, one vertical one, and one exit for the ion beams. The bending radius of the magnet BMR40 is equal to 40 cm. The maximum magnetic field corresponds to 0.75 kG, gap height is 70 mm. The maximum magnetic field of the solenoids does not exceed 3 kG, a good field region is of 80 mm. The maximum quadrupole lens gradient does not exceed 100 G/cm.

The big values of the magnetic field from the C400 cyclotron in the region of the horizontal part of the channel and inside the BMR40 and the quadrupole lens require an additional shielding.

The simulation of the ion beam transportation has been made. For all types of ions the beam diameters at the entrance into the spiral inflector are smaller than 2 mm.

A model of the dee geometry at the cyclotron center with the inflector housing was developed. Dee tips have the vertical aperture 1.2 cm in the first turn and 2 cm in the second and further turns. In the first turn the gaps were delimited with pillars reducing the transit time. The azimuth extension between the middles of the accelerating gaps was chosen to be 45°. The electric field simulation of the central region was performed. The electric field in the inflector was chosen to be 20 kV/cm. Thus, the height (electric radius) of the inflector (Fig. 3) is 2.5 cm. The gap between electrodes was taken to be 6 mm, tilt parameter is equal to k′=0.1. The aspect ratio between the width and the spacing of the electrodes was taken to be 2 to avoid the fringe field effect.
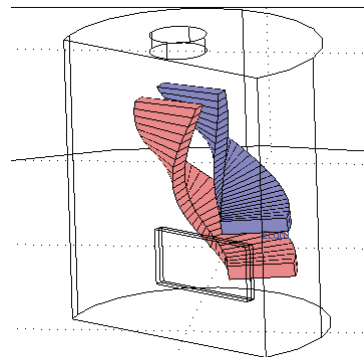


Figure 3: The spiral inflector k′=0.1 E=20 kV/cm.

Beam dynamics simulations were made for particles with initial distributions in transverse phase planes obtained from the axial injection line. The inflector with tilt k′=0.1 can be effectively used for beam intensity modulation. Axial beam motion is given in Fig. 4. Fig. 5 demonstrates turns in the central region for design voltage $U_0 = \pm5.82$ kV (100% intensity - green lines), for $U=0.95U_0$ (53% intensity - blue lines) and for $U=0.9U_0$ (15% intensity - red lines). The voltage $0.89U_0$ corresponds to the situation when all beam is lost in the diaphragm (situated on the first antidee - 0.2 mm).
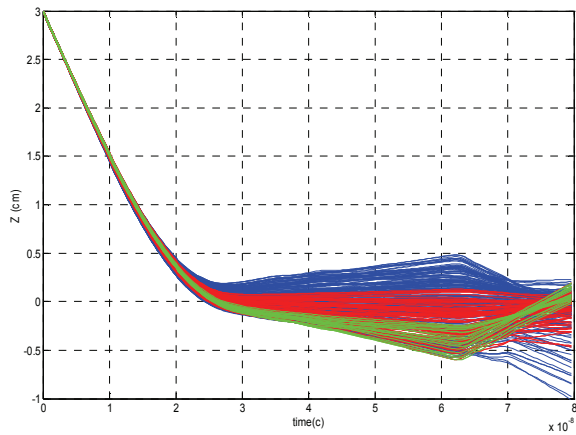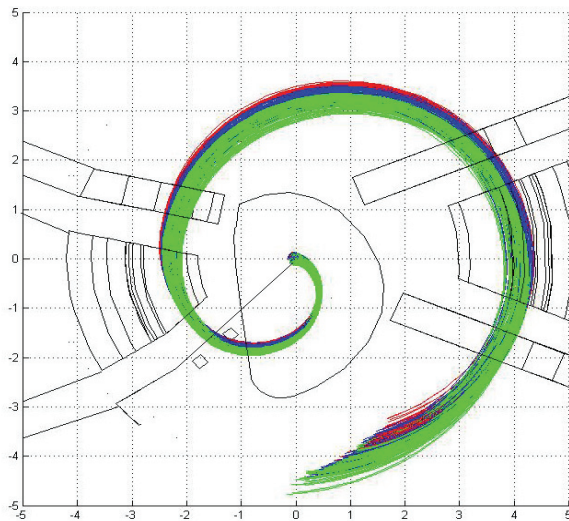
Figure 4: Axial beam motion.



Figure 5: First turns in the center region.

## MAGNET SYSTEM

The simulation and design of the C400 magnetic system was based on its main characteristics: four-fold symmetry and spiral sectors; deep-valley concept with RF cavities placed in the valleys; elliptical pole gap is 120 mm at the center decreasing to 12 mm at extraction; accelerate up to 10 mm from the pole edge to facilitate extraction; pole radius is 187 cm; hill field is 4.5 T, valley field is 2.45 T; magnetic induction inside yoke is less 2-2.2 T; the magnet weight is 700 tons and the magnet yoke diameter is 6.6 m; the main coil current is 1.2 MA. The main parameters of the cyclotron magnetic system were estimated and optimized by computer simulation with the 3D TOSCA code (Fig. 6).

The view of the spiral sectors is given in Fig. 6. The sectors are designed by a way with flat top surface and without additional grooves, holes etc. The sectors have the following parameters: the initial spiral law with parameter $N\lambda=77$ cm with increasing spiral angle to the final radius with parameter $N\lambda\sim55$ cm; the sectors azimuth width is varying from 25° in the cyclotron center to 45° at the sectors edge; axial profile is the ellipse with

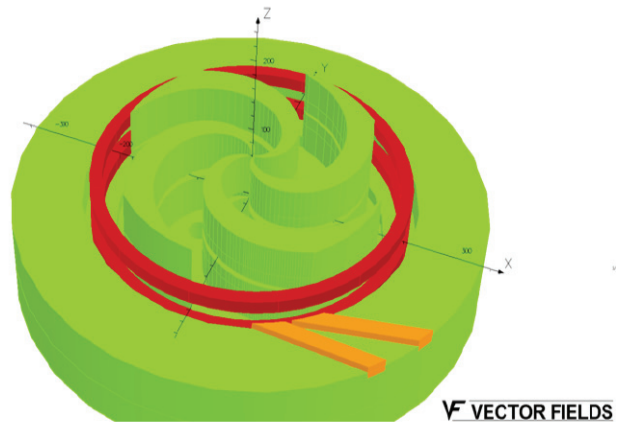60/1874 mm semi-axis, at the final radii the ellipse axial profile is cut by the planes at the distance z= ± 6 mm.



Figure 6: 3D TOSCA simulation of C400 magnetic system.

The accuracy of average magnetic field at shaping simulation is ±10 G in the middle and end region of the beam acceleration. The required isochronous magnetic field was shaped by azimuth profiling of the sectors. The optimized sector geometry provides vertical focusing $Q_z\sim$ 0.4 in the extraction region (Fig. 7).
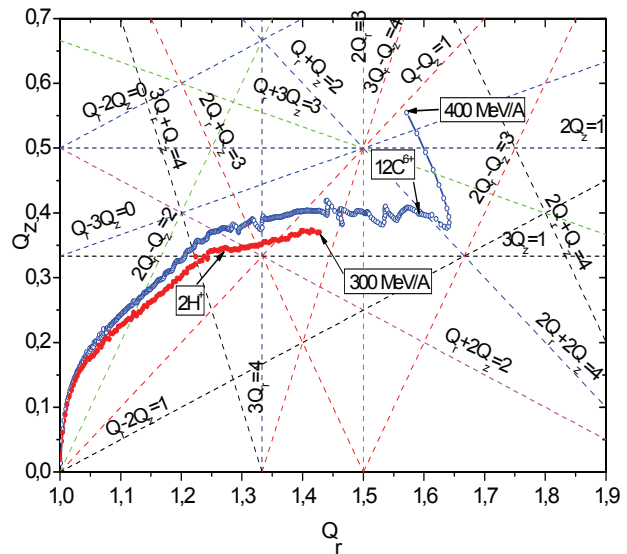


Figure 7: Working diagram of the cyclotron.

## ACCELERATING SYSTEM

Acceleration of the beam will occur at the fourth harmonic of the orbital frequency, i.e. at 75 MHz. The acceleration will be obtained through two cavities placed in the opposite valleys. Two 45° dees working at the fourth harmonic will guarantee the maximum acceleration. The dee voltage increases from 80 kV at the center to 170 kV in the extraction region. A geometric model of the double gap delta cavity housed inside the valley of the magnetic system was developed in the Microwave Studio (Fig. 8).
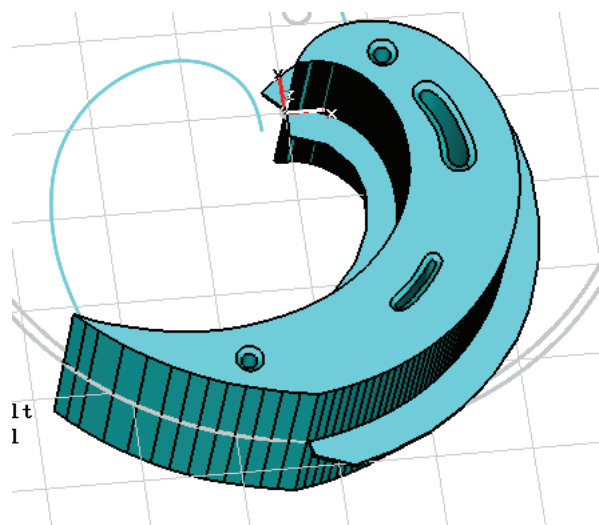
Figure 8: View of RF cavity model.

The depth of the valley permits accommodation of the cavity with total height 116 cm. The vertical dee aperture was equal to 2 cm. The accelerating gap was 6 mm at the center and 80 mm in the extraction region. The distance between the dee and the back side of the cavity was 45 mm. The azimuth extension of the cavity (between the middles of the accelerating gaps) was 45º up to the radius 150 cm. The cavities have a spiral shape similar to the shape of the sectors. We inserted four stems with different transversal dimensions in the model and investigated different positions of the stems to ensure increasing voltage along the radius. The thickness of the dee was 20 mm. Edges of the dees are 10 mm wide. Basing on the 2D electric field simulations we have chosen the optimal form of the dee edges. RF heating simulation was performed to determine the cooling system layout.

Each cavity will be excited with the RF generator through a coupling loop (which should be rotated azimuthally within small limits). For precise resonator adjustment, a tuner (piston) will be provided at radii compatible with the holes in the yoke. Average losses will be about 50 kW. Each cavity will be powered by a 75 MHz 100 kW tetrode-based amplifier (as used in the current C235 cyclotron).

## ION DYNAMICS

During a whole range of acceleration the carbon beam crosses the lines of 15 resonances up to 4th order (Table 2). The working diagrams presented in Fig. 7 have been computed via an analysis [3] of the small oscillations around the closed orbits. All resonances can be subdivided into two groups. The first group consists of 6 internal resonances ($nQ_r \pm kQ_z = 4$, n, k=0, 1, 2, 3, 4, $n+k\leq4$) having the main 4th harmonic of the magnetic field as a driving term. The second group includes 11 external resonances ($nQ_r \pm kQ_z = m$, m=0, 1, 2, 3) that could be excited by the magnetic field perturbations.

Requirements to the field imperfections imposed by the dangerous resonances will be able to be provided in practice at today's level of cyclotron technology.

Table 2: List of Resonances up to 4th Order

| Resonance, (Level of Danger) | Radius (cm) (Driving Term) | Description, tolerances |
|---|---|---|
| $Q_r = 1$ (Yes) | 2-10 ($B_{z1}$) | Increase in radial amplitudes $B_{z1} <$ 2-3 G |
| $4Q_r = 4$ (Not) | 2-10 ($B_{z4}, \varphi_{z4}$) | Weak influence on radial motion at acceleration |
| $2Q_r - Q_z = 2$ (Not) | 110 ($B_{z2}, B_{r2}$) | Increase in axial amplitudes $B_{z2} <$ 200 G, $B_{r2} <$ 50 G |
| $3Q_r + Q_z = 4$ (Not) | 131 ($B_{z4}, \varphi_{z4}$) | No influence up to $A_z$, $A_r = 5$-7 mm |
| $Q_r - Q_z = 1$ (Yes) | 145 ($B_{r1}$) | Increase in axial amplitudes $B_{r1} <$ 5-7 G |
| $3Q_r = 4$ (Yes) | 154 ($B_{z4}, \varphi_{z4}$) | Increase in radial amplitudes beginning from $A_r = 1.5$ mm. Can be corrected by average field perturbation. |
| $2Q_r + Q_z = 3$ (Not) | 157 ($B_{r3}$) | Increase in axial amplitudes $B_{r3} <$ 10 G |
| $Q_r + 2Q_z = 2$ (Not) | 162 ($B_{z2}$) | Increase in axial amplitudes $B_{z2} <$ 20 G |
| $3Q_z = 1$ (Not) | 167 ($B_{r1}$) | Increase in axial amplitudes $B_{r1} <$ 20 G |
| $3Q_r - Q_z = 4$ (Not) | 167 ($B_{z4}, \varphi_{z4}$) | Increase in radial amplitudes. No influence if no axial amplitudes increase on resonance $3Q_z = 1$ due to $B_{r1}$ |
| $2Q_r = 3$ (Not) | 172 ($B_{z3}$) | Increase in radial amplitudes $B_{z3} <$ 10 G |
| $Q_r + Q_z = 2$ (Not) | 177 ($B_{z2}, B_{r2}$) | Increase in radial and axial amplitudes $B_{r2} <$ 10 G |
| $2Q_r + 2Q_z = 4$ (Not) | 177 ($B_{z4}, \varphi_{z4}$) | No influence |
| $Q_r + 3Q_z = 3$ (Not) | 179 ($B_{z3}$) | Increase in axial amplitudes $B_{z3} <$ 10 G |
| $2Q_r - Q_z = 3$ (Not) | 180 ($B_{z3}$) | Increase in axial amplitudes $B_{z3} <$ 10 G |
| $2Q_r + Q_z = 4$ (Not) | 181 ($B_{z4}, \varphi_{z4}$) | Increase in axial amplitudes. Requires proper deflector positioning. |
| $2Q_z = 1$ (Yes) | 181 ($B_{z1}, B_{r1}$) | Increase in axial amplitudes $B_{r1} <$ 10 G, $dB_{z1}/dr <$ 1 G/cm |

## EXTRACTION

Extraction of protons is supposed to be done by means of the stripping foil. It was found that 320 MeV is the minimal attainable energy of protons which can be extracted during 1-turn after the stripping foil and 265 MeV is the minimal energy of protons for 2-turns

extraction (Fig. 8). This variant was chosen as optimal one because the energy of the 2-turns extracted protons is essentially closer to the normally used energy for the proton beam treatment. The radius of foil in this case is 161.3 cm, azimuth is 51°.
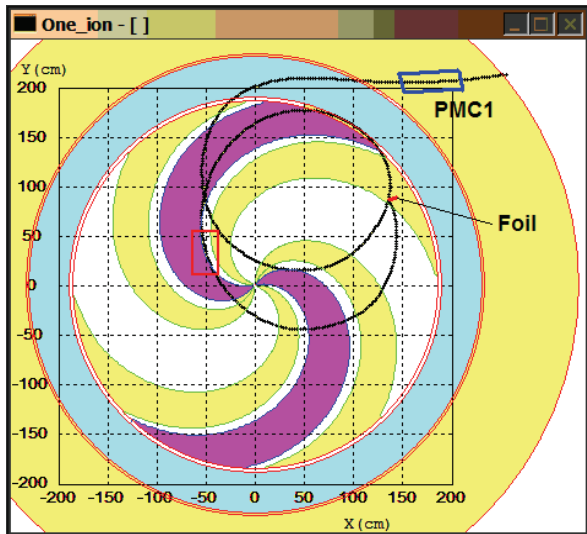


Figure 8: Extraction of proton with energy 265 MeV.

It is possible to extract the carbon beam by means of one electrostatic deflector (which is located in valley between sectors) with a 150 kV/cm field inside. Septum of the deflector was located at the radius 179.7 cm for tracking simulation. The extraction efficiency was estimated as 73% for the septum with increased $(0.1 - 2)$ mm thickness along its length. The extraction of the carbon and proton beams by the separate channels and their further alignment by the bending magnets outside the cyclotron was chosen as the acceptable variant. The passive magnetic elements (correctors) are supposed to be used inside the cyclotron and the active current elements (quadrupole lenses and bending magnets) outside the yoke. A plan view of both lines is shown in Fig. 9. The system for carbon ion extraction consists of the electrostatic deflector, two passive magnetic correctors MC1,2, three quadrupole lenses CQL1−3 and two steering dipole magnets CSM1-2. Proton beam extraction system consists of the stripping foil, magnetic corrector PMC1, two bending magnets BM1-2, two quads PQL1-2 and two steering magnets PSM1-2.

Modeling of the different focusing elements action in both carbon and proton extraction systems was carried out to avoid the beams large divergence during the extraction (Fig. 10). It is possible to align both beams into one direction just before the energy degrader (6750 mm from the cyclotron center). Both beams have a spot with $\sigma_{x,y} < 1$ mm at this point. Transverse emittances are equal to $10\ \pi$ mm·mrad and $4\pi$ mm·mrad for the extracted carbon beam.
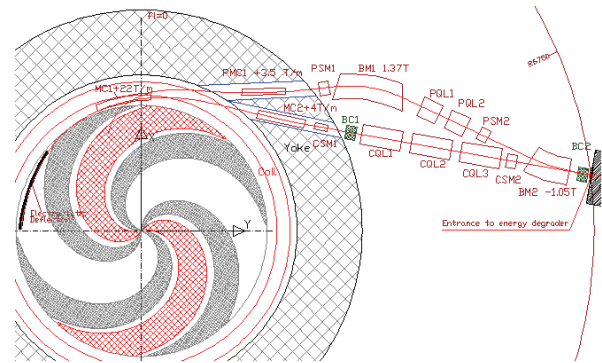


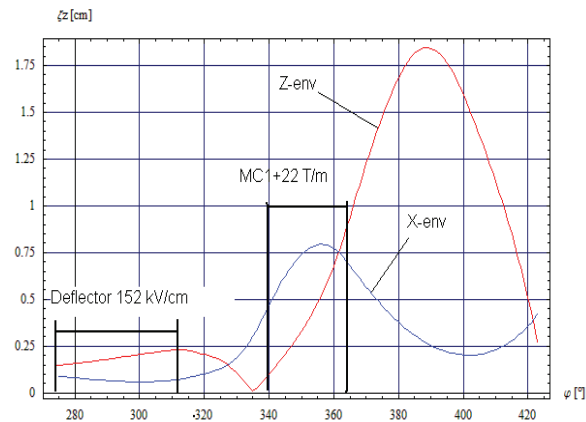Figure 9: Layout of the cyclotron C400 with two extraction lines.



Figure 10: Carbon envelopes (2σ) inside the cyclotron. Deflector with uniform electric field is used.

## CONCLUSIONS

The detailed computer simulations of the beam dynamics and the main systems of C400 cyclotron have been performed. The results of the simulations show that the energy range up to 400 MeV/amu (K = 1600) can be achieved with the compact design similar to that of the existing IBA C235 cyclotron. The C400 cyclotron will also provide a proton therapy beam with energy 265 MeV.

## REFERENCES

[1] Y. Jongen et al., "Design Studies of the Compact Superconducting Cyclotron for Hadron Therapy", in Proc. of EPAC 2006, Scotland, p. 1678.

[2] Y. Jongen et al., "IBA C400 Cyclotron Project for hadron therapy", in Proc. of Cyclotrons 2007, p. 151.

[3] Y. Jongen et al., "Numerical study of the resonances in superconducting cyclotron C400", in Proc. of Cyclotrons 2007, p. 382.

[4] Y. Jongen et al, "Current status of the IBA C400 cyclotron project for hadron therapy", in Proc. of EPAC 2008, p. 1806.